Quadruped Jumping via Adaptive Contact and Frequency Control

Jaeyoon Kim and Dr. Jaemin Lee

Department of Mechanical and Aerospace Engineering

NC STATE UNIVERSITY

HIER LAB

Motivation

*How can we design more **reliable, efficient, and consistent** jumping behaviors in quadruped robots—suitable for dynamic and unpredictable environments?*

Challenge

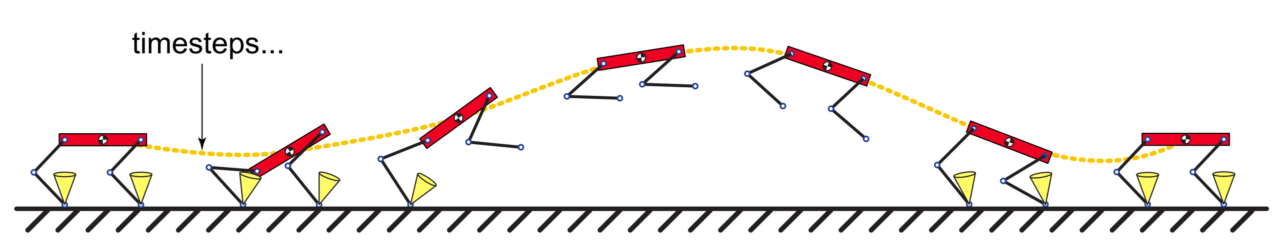

(1) The baseline trajectory optimization approach for dynamic jumping is computationally expensive because it involves solving a large, nonlinear, constrained optimization problem over a continuous-time system that must be discretized into multiple timesteps.

(2) Using unsuitable jumping sequence schedule with fixed andinappropriate timelines for different jump types leads to robot motions that lack adaptability, thereby limiting performance and robustness across various tasks and environments.

Hypothesis:

Adaptive contact planning combined with a **variable-frequency horizon** in trajectory optimization (TO) can produce more effective trajectory references that improve stability, height, and distance, while **improving computational efficiency** for downstream predictive control execution.

Robot Model

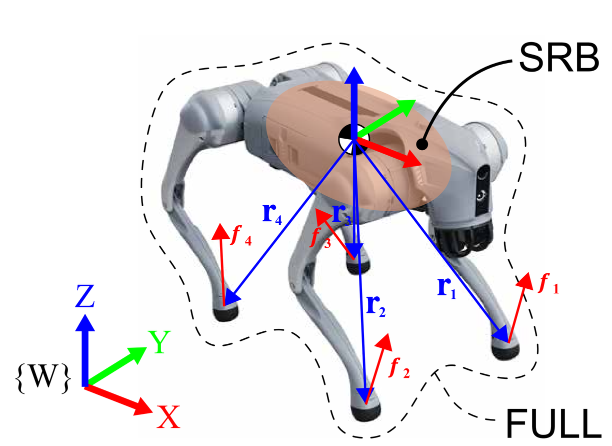

In this work, we introduce two models of the robot. The robot is modeled as a single rigid body (SRB) for contact timing optimization, simplifying the complex full-body dynamics. A full rigid body system is then used for full-body TO to capture dynamics.

Reduced-order model:

The SRB's equations of motion are Cartesian space can be derived as:

$$\ddot{\boldsymbol{p}} = \sum_{s=1}^{n_s} \boldsymbol{f}_s / m - \boldsymbol{g}$$

$$\boldsymbol{I}_b \dot{\boldsymbol{\omega}} + \boldsymbol{\omega} \times (\boldsymbol{I}_b \boldsymbol{\omega}) = \sum_{s=1}^{n_s} (\boldsymbol{p} - \boldsymbol{p}_f^s) \times \boldsymbol{f}_s$$

$$\dot{\boldsymbol{R}} = \boldsymbol{R}\hat{\boldsymbol{\omega}}$$

n_s	number of contact feet
m	robot's mass
g	gravity acceleration
$\boldsymbol{\omega} \in \mathbb{R}^3$	angular acceleration of the body in the world frame
$\boldsymbol{R}$	rotation matrix of the body frame
$\boldsymbol{p}, \dot{\boldsymbol{p}}, \ddot{\boldsymbol{p}} \in \mathbb{R}^3$	CoM position, velocity, acceleration of the body in the world frame
$\boldsymbol{f}_s \in \mathbb{R}^3$	ground reaction force on s^{th} foot
$\boldsymbol{p}_f^s \in \mathbb{R}^3$	s^{th} foot position in the world frame

Full-body dynamics:

$$\begin{bmatrix} \boldsymbol{M} & -\boldsymbol{J}_s^T \\ -\boldsymbol{J}_s & 0 \end{bmatrix} \begin{bmatrix} \ddot{\boldsymbol{q}} \\ \boldsymbol{F}_s \end{bmatrix} = \begin{bmatrix} -\boldsymbol{C}\dot{\boldsymbol{q}} - \boldsymbol{G} + \boldsymbol{B}\boldsymbol{\tau} \\ \dot{\boldsymbol{J}}_s \dot{\boldsymbol{q}} \end{bmatrix}$$

$\boldsymbol{M}$	mass inertia matrix
$\boldsymbol{C}$	Coriolis and centrifugal terms
$\boldsymbol{G}$	gravity vector
$\boldsymbol{B}$	actuator distribution matrices
$\boldsymbol{\tau}$	actuator torque
$\boldsymbol{F}_s$	contact forces at the s^{th} contact foot
$\boldsymbol{J}_s$	contact Jacobian of the body containing s^{th} contact foot

$\boldsymbol{q} \coloneqq [\boldsymbol{q}_b; \boldsymbol{q}_j]$	vector of generalized coordinates
$\dot{\boldsymbol{q}}, \ddot{\boldsymbol{q}}$	corresponding velocity and acceleration

$\boldsymbol{q}_b \in \mathbb{R}^6$	body position and orientation
$\boldsymbol{q}_j \in \mathbb{R}^{12}$	joint angles vector

System Architecture

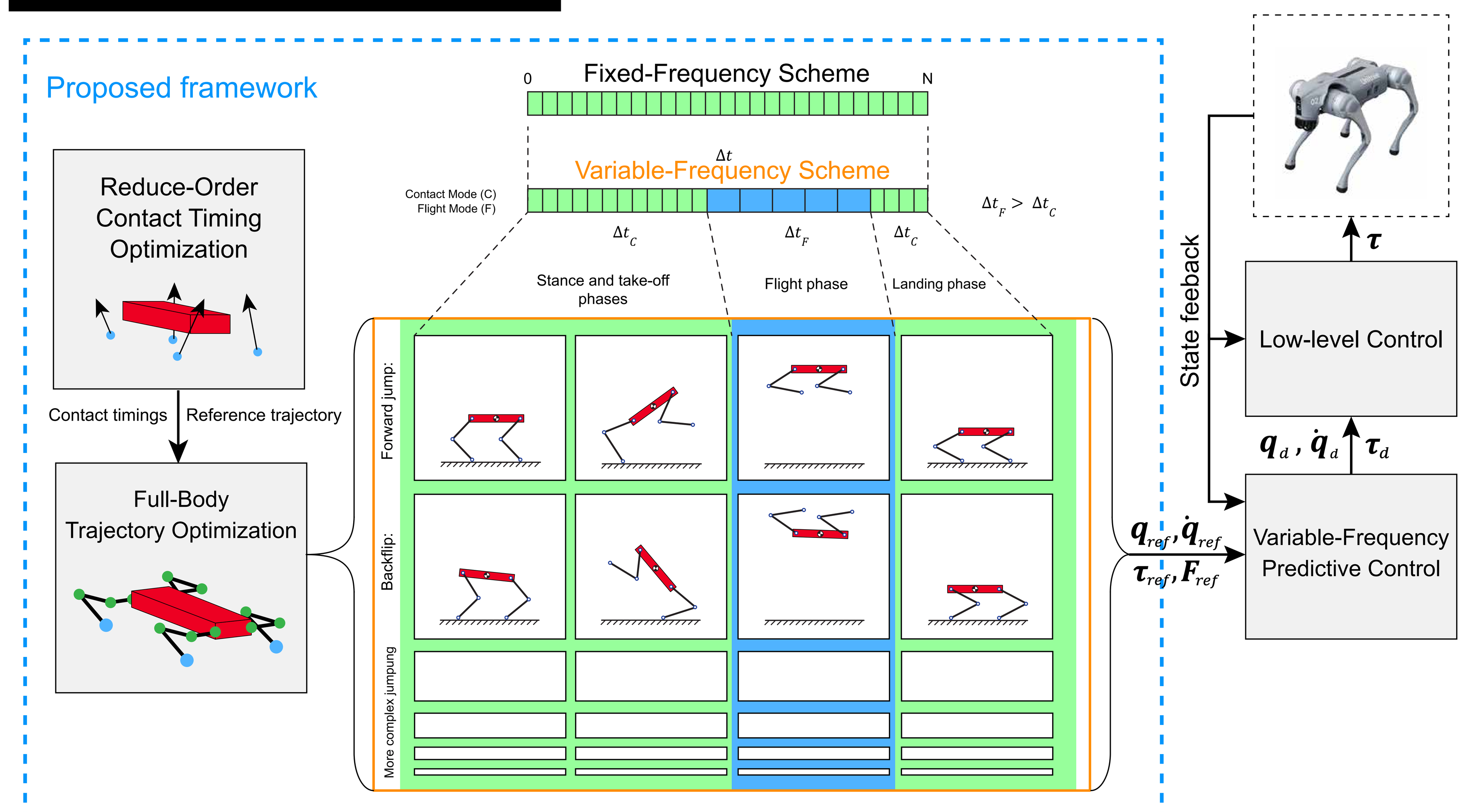

A reduced-order model is used to optimize contact timing, yielding phase durations and a CoM trajectory. These inform a full-body trajectory optimization that solves for reliable feedforward trajectory references for downstream predictive control execution, using variable-frequency timesteps with matching integration steps, a variable-frequency horizon, and the predefined contact schedule.

Design Optimization

Contact timings optimization:

$$\underset{\boldsymbol{x},\boldsymbol{f}}{\text{minimize}} \sum_{k=1}^{N} \epsilon_\omega \boldsymbol{\omega}_k^T \boldsymbol{\omega}_k + \epsilon_f \boldsymbol{f}_k^T \boldsymbol{f}_k$$

s.t.

$[\boldsymbol{R}, \boldsymbol{p}, \boldsymbol{p}_f^s](k=1) = [\boldsymbol{R}_0, \boldsymbol{p}_0, \boldsymbol{p}_{f,0}^s]$,	*initial states*
$[\boldsymbol{\Omega}, \dot{\boldsymbol{\Omega}}, \dot{\boldsymbol{p}}](k=1) = \boldsymbol{0}$,	*initial states*
$[\boldsymbol{R}, \boldsymbol{p}, \boldsymbol{p}_f^s](k=N^c) = [\boldsymbol{R}_g, \boldsymbol{p}_g, \boldsymbol{p}_{f,g}^s]$,	*final states*
$\lvert \boldsymbol{R}(k)[\boldsymbol{p}_f^s(k) - \boldsymbol{p}(k)] - \bar{\boldsymbol{p}}_f^s(k) \rvert \leq \mathbf{r}$,	*foot position*
$\lvert \boldsymbol{f}_k^{s,x} / \boldsymbol{f}_k^{s,z} \rvert \leq \mu, \lvert \boldsymbol{f}_k^{s,y} / \boldsymbol{f}_k^{s,z} \rvert \leq \mu$,	*friction cone*
$\boldsymbol{f}_{k,min}^s \leq \boldsymbol{f}_k^{s,z} \leq \boldsymbol{f}_{k,max}^s$,	*GRF limits*
$\boldsymbol{p}_{k,min} \leq \boldsymbol{p}_k \leq \boldsymbol{p}_{k,max}$,	*CoM limits*
$\sum_{i=1}^{n_p} T_i \in [T_{min}, T_{max}]$	*timings limit*

Solving for the optimal contact timings and reference trajectory to generate **a safe and adaptable jumping sequence** for any desired jump, enabling motion flexibility across various tasks and environments.

$\epsilon_\omega, \epsilon_f$	cost function weights for corresponding terms
$\mathbf{r}$	relative position between CoM and foot
μ	friction coefficient
n_p	number of phases

Full-body trajectory optimization:

$$J = \sum_{h=1}^{N-1} \epsilon_q (\boldsymbol{q}_h - \boldsymbol{q}_{ref,h})^T (\boldsymbol{q}_h - \boldsymbol{q}_{ref,h}) + \epsilon_{\dot{q}} (\dot{\boldsymbol{q}}_h - \dot{\boldsymbol{q}}_{ref,h})^T (\dot{\boldsymbol{q}}_h - \dot{\boldsymbol{q}}_{ref,h}) + \epsilon_\tau \boldsymbol{\tau}_h^T \boldsymbol{\tau}_h$$

s.t. *Full-body dynamics constraints from 1),*

**Euler integration*

$\boldsymbol{q}(h=0) = \boldsymbol{q}_0, \ \dot{\boldsymbol{q}}(h=0) = 0$	*initial configuration*
$\boldsymbol{q}(h=N) = \boldsymbol{q}_N, \ \dot{\boldsymbol{q}}(h=N) = 0$	*final configuration*
$\boldsymbol{q}_{j,min} \leq \boldsymbol{q}_j \leq \boldsymbol{q}_{j,max}$	*joint angle constraints*
$\lvert \dot{\boldsymbol{q}}_{j,h} \rvert \leq \dot{\boldsymbol{q}}_{j,max}$	*joint velocity constraints*
$\lvert \boldsymbol{\tau}_h \rvert \leq \boldsymbol{\tau}_{max}$	*joint torque limits*
$\lvert \boldsymbol{F}_h^x / \boldsymbol{F}_h^z \rvert \leq \mu, \ \lvert \boldsymbol{F}_h^y / \boldsymbol{F}_h^z \rvert \leq \mu$,	*friction cone limits*
$\boldsymbol{F}_h^z \geq \boldsymbol{F}_{min}^z$	*minimum GRF*

Kinematics constraints to guarantee: (i) each robot part does not collide with others, (ii) the whole robot body and legs have a good clearance with obstacle.

$\epsilon_q, \epsilon_{\dot{q}}, \epsilon_\tau$	cost function weights
μ	friction coefficient

*Euler integration approximates how the robot's state evolves over time at different phase mode:

$$\text{at flight mode} \begin{cases} \boldsymbol{q}_{h+1} = \boldsymbol{q}_h + \dot{\boldsymbol{q}}_h \Delta \boldsymbol{t}_C \\ \dot{\boldsymbol{q}}_{h+1} = \dot{\boldsymbol{q}}_h + \ddot{\boldsymbol{q}}_h \Delta \boldsymbol{t}_C \end{cases}$$

$$\text{at contact mode} \begin{cases} \boldsymbol{q}_{h+1} = \boldsymbol{q}_h + \dot{\boldsymbol{q}}_h \Delta \boldsymbol{t}_F \\ \dot{\boldsymbol{q}}_{h+1} = \dot{\boldsymbol{q}}_h + \ddot{\boldsymbol{q}}_h \Delta \boldsymbol{t}_F \end{cases}$$

Results

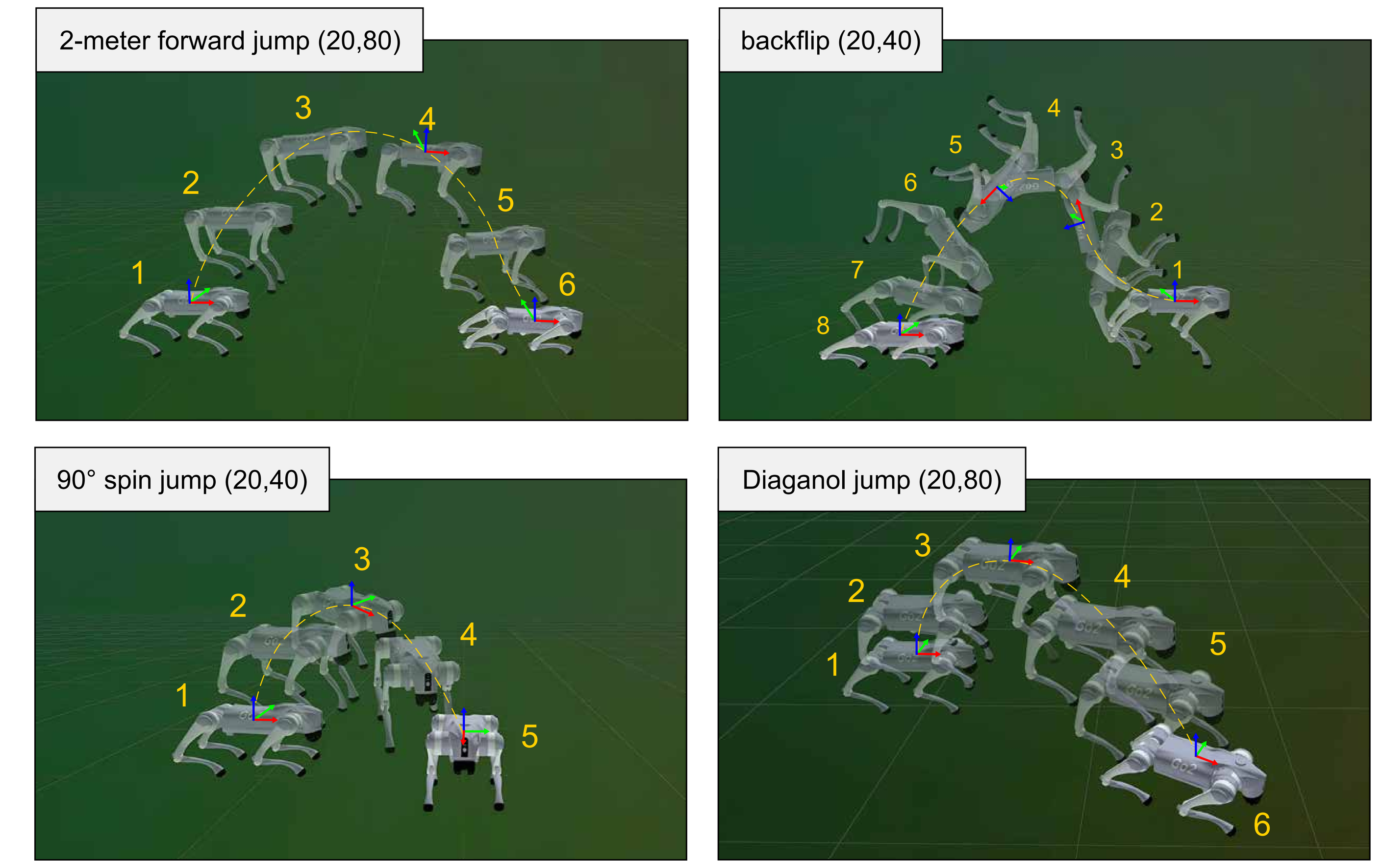

The results of our TO approach were validated by visualizing the solved trajectories on a model of the Unitree Go2 quadruped robot. Used variable-frequency time horizon is denoted as $(\Delta t_C, \Delta t_F)$.

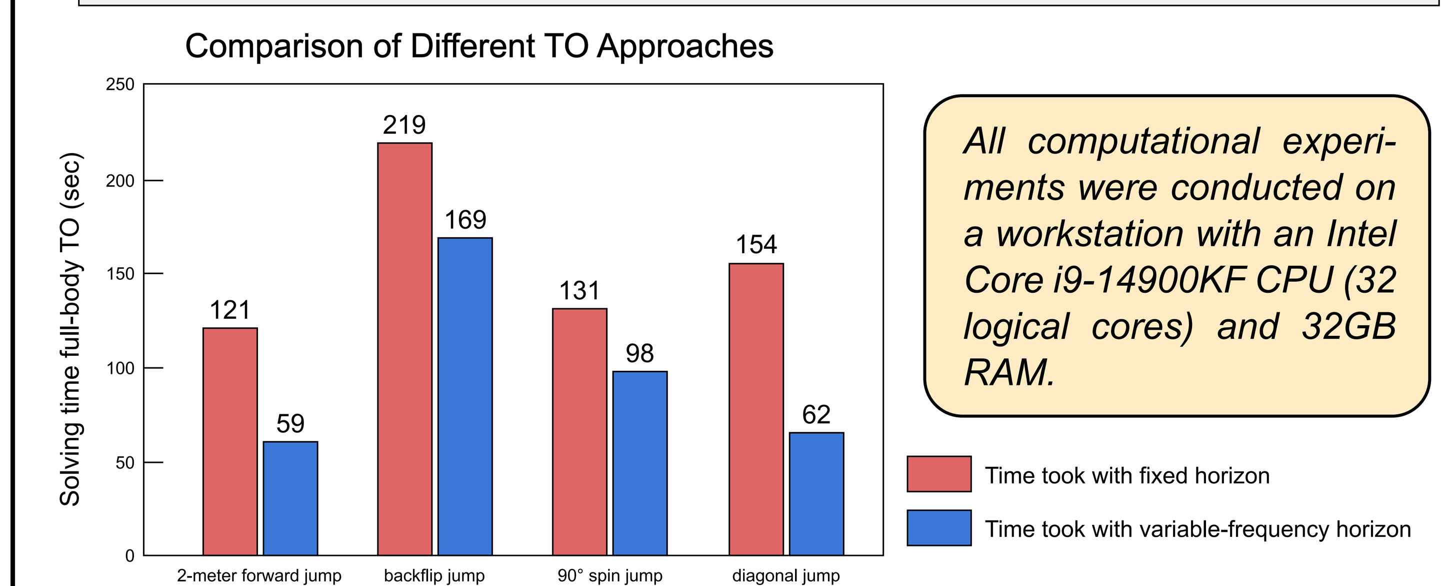

All computational experiments were conducted on a workstation with an Intel Core i9-14900KF CPU (32 logical cores) and 32GB RAM.

- ***Contact timing** enhanced the planning of adaptive contact sequences, **providing more stable and safer solution**.*
- *The proposed full-body trajectory optimization method using a variable-frequency horizon **reduced the solving time by an average of 39.8 %** across the four types of jumps experimented, significantly reducing the computational cost.*
- *A key finding is that the variable-frequency approach becomes **increasingly effective for jumps with longer flight times**.*

Future Works

Fast Optimization and Learned Dynamics Model:

Planning highly dynamic jumping maneuvers remains computationally intensive. To address this, future work will focus on finding faster optimization methods and incorporating learned dynamics models to improve accuracy upon execution.

Sequential Contact Jumping Motion Planning:

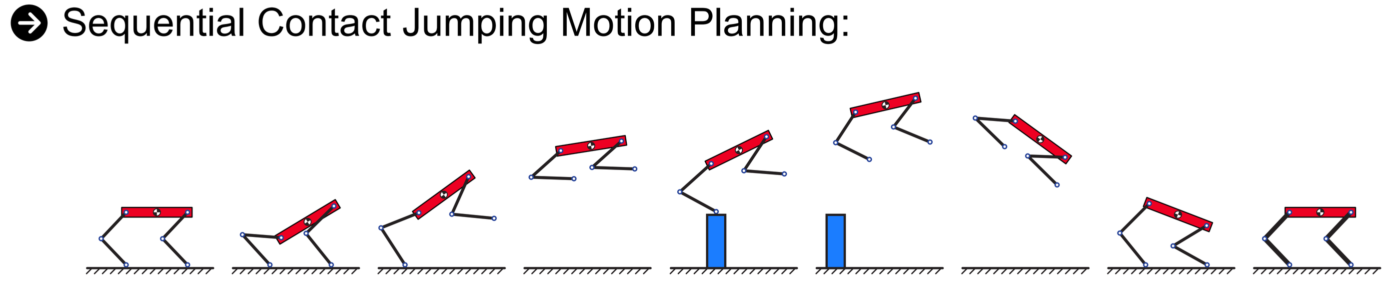

Our goal is to advance from single-jump optimization to robust planning for sequential contact jumping, allowing multiple contact transitions—such as jumping onto, over, or off obstacles of varying height and orientation, including vertical surfaces—by fully exploiting the robot's contact coordination and contact versatility.